Pakistan Veterinary Journal

ISSN: 0253-8318 (PRINT), 2074-7764 (ONLINE)
DOI: 10.29261/pakvetj/2026.170

RESEARCH ARTICLE

Evaluation of the Impact of *Cryptosporidium* Infection on the Fungi in the Intestines of Yaks

Bin Shi[1,2*], Chang Xu[3], Cidanzhuoga[1] and Mikhlid H. Almutairi[4]

[1]Institute of Animal Husbandry and Veterinary Medicine, Xizang Academy of Agricultural and Animal Husbandry Sciences, Lhasa 850009, China; [2]Key Laboratory of Animal Parasitology of Xizang, Institute of Animal Husbandry and Veterinary Medicine, Xizang Academy of Agricultural and Animal Husbandry Sciences, Lhasa 850009, China; [3]College of Veterinary Medicine, Nanjing Agricultural University, Nanjing 210095, China; [4]Department of Zoology, College of Science, King Saud University, P.O. Box 2455, Riyadh 11451, Saudi Arabia
*Corresponding author: sapstone@163.com

ARTICLE HISTORY (26-711)

Received: June 9, 2026
Revised: July 20, 2026
Accepted: July 23, 2026
Published online: July 28, 2026

Keywords:
Cryptosporidium
Intestinal fungus
Yak
Parasite

ABSTRACT

Cryptosporidium is one of the six major pathogens causing diarrhea worldwide, and it poses many hazards. To study the effect of *Cryptosporidium* infection on the intestinal fungal community of the host, this study focused on yaks and collected fecal samples from the infected group (CP, n=6) and the control group (CO, n=6). The structure and composition of the intestinal fungal community were analyzed using ITS amplicon sequencing technology. A significant decline in fungal diversity and evenness after infection was indicated by results showing that the Shannon index, Simpson index, and Pielou evenness of the infected group were significantly lower than those of the control group ($P<0.05$). Beta diversity analysis (PCoA, NMDS, and UPGMA clustering tree) revealed that the two groups of samples could be clearly separated, and the samples of the infected group were more closely clustered. Both groups were dominated at the phylum level, and these are Ascomycota and Basidiomycota, but the relative abundance of the Ascomycota phylum in the infected group (79.09%) was higher than that in the control group (64.82%). At the class level, the infected group enriched Leotiomycetes and Tremellomycetes. At the order level, Thelebolales (61.57%) and Filobasidiales (18.60%) were dominant in the infected group, while Pleosporales (39.57%) and Coniochaetales (6.27%) were dominant in the control group. At the genus level, *Naganishia* (46.84%) was significantly enriched in the infected group, while *Neoascochyta* (6.86%), *Neostagonospora* (5.69%), and others were higher in the control group. LDA analysis and the Wilcox test further confirmed the statistical significance of the above differential taxonomic units. *Cryptosporidium* infection can significantly alter the variety and composition of the intestinal fungal community, forming a fungal structure characterized by the amplification of opportunistic fungi such as *Naganishia*.

To Cite This Article: Shi B, Xu C, Cidanzhuoga, Almutairi MH, 2026. Evaluation of the impact of *Cryptosporidium* infection on the fungi in the intestines of yaks. Pak Vet J, 46(7): 1772-1781. http://dx.doi.org/10.29261/pakvetj/2026.170

INTRODUCTION

Yak is a unique livestock species specific to the Qinghai-Xizang Plateau, which is not only an essential production and living resource for the local herders but also an important component of the alpine grassland ecosystem (Shah *et al.*, 2023; Ji *et al.*, 2025). The development of yak farming has long been plagued by various parasitic diseases, among which cryptosporidiosis caused by *Cryptosporidium* spp. is particularly prominent (Budu-Amoako *et al.*, 2011; Adkins, 2022). *Cryptosporidium* is a globally distributed intestinal protozoan that can infect 260 different species of vertebrates, including humans (Bouzid *et al.*, 2013; Shehata *et al.*, 2024). It can cause persistent diarrhea and even death in calves and immunocompromised hosts (Harp, 2003). Epidemiological surveys have shown that the infection of *Cryptosporidium* in yaks is relatively common, with infection rates fluctuating between 1.0 and 13.2% in different regions (Geng *et al.*, 2021; Peng *et al.*, 2024). The main species include *C. bovis*, *C. andersoni*, and *C. ryanae*, etc. In recent years, human-borne *Cryptosporidium* species and genotypes have been detected in yaks and are considered a potential threat to public health safety (Guo *et al.*, 2022; Alberfkani *et al.*, 2024).

The relationship between intestinal microbiota and the host has received increased attention with the rapid development of microbiome technology (Hertli and Zimmermann, 2022; Ignatiou and Pitsouli, 2024). As an important component of the intestinal system, although fungi are far outnumbered by bacteria in quantity, they play an irreplaceable role in nutrient metabolism, immune regulation, and maintaining intestinal homeostasis (Chen *et al.*, 2024; Lin *et al.*, 2025). Studies have revealed that dysregulation of the intestinal fungal community is closely linked to the occurrence and development of inflammatory bowel disease, metabolic syndrome, and various infectious diseases (Lin *et al.*, 2025; Soliman *et al.*, 2025). Intestinal protozoan infections can significantly alter the intestinal microenvironment of the host (Hatter *et al.*, 2018). For *Cryptosporidium*, studies have confirmed that its infection can lead to changes in the composition and diversity of the host's intestinal bacterial community (Xu *et al.*, 2025). However, research on how *cryptosporidium* infection affects the intestinal fungal community is very limited.

Research on *Cryptosporidium* in yaks has mainly focused on epidemiological investigations, species identification, and genotyping, with relatively few studies exploring the changes in the intestinal microecology of the host after infection. Only limited studies have preliminarily discovered the impact of *Cryptosporidium* infection on the intestinal microbiota of yaks, finding that the diversity and compositional structure of the microbiota in infected individuals have undergone significant changes (Ichikawa-Seki *et al.*, 2019; Lu *et al.*, 2023). The abundance of some opportunistic pathogens has increased, while certain beneficial bacteria have been inhibited. A previous study conducted a comparison of the differences in fungal communities of *Cryptosporidium-infected* yak fecal samples. Between the infected and control groups, significant differences in the relative abundance of two fungal phyla and 21 fungal genera were observed (Lu *et al.*, 2023). A significant decrease in concentrations of key metabolites such as propionic acid, acetic acid, and butyric acid occurs when *Cryptosporidium* infection leads to a comprehensive disruption of the yak intestinal microecosystem. Dong *et al*. (2023) also focused on the changes in bacterial communities and short-chain fatty acids. In addition to the direct damage caused by the parasite, disrupting the intestinal fungal homeostasis may also be an important way for it to cause digestive disorders and diarrhea in the host. It is worth noting that existing studies have shown that environmental factors, rearing methods, and common diarrhea can significantly alter the structure of the intestinal fungal community in yaks (Wang and Zeng, 2026). This study collected fecal samples from yaks on a certain natural pasture in multiple regions, identified positive and negative individuals with *Cryptosporidium* infection, and used high-throughput sequencing technology in the ITS region to compare diversity, composition, and structural differences of intestinal fungal communities of two groups of samples. It revealed the specific impact of *Cryptosporidium* infection on the fungal community and screened out the differential fungal groups related to the infection status.

MATERIALS AND METHODS

Sample collection: This study conducted sample collection at a natural pasture on the Qinghai-Xizang Plateau. The average altitude of this area is over 3500 meters. During the sampling process, for each yak, the feces that did not come into contact with the ground were immediately collected using a sterile sampling spoon to avoid contamination by environmental fungi. Approximately 50-100 grams of each sample were collected, placed in sterile sampling bags, sealed, and labeled with information such as the sample number, sampling date, and estimated age. A total of 20 samples of healthy yak feces (without diarrhea) and 31 samples of diarrhea yak feces were collected. Fecal samples without diarrhea were classified into the CO group if no *Cryptosporidium* was detected by PCR, while those with diarrhea and C*ryptosporidium* present in the diarrhea feces were classified into the CP group. All samples were stored in portable ice boxes (at 4°C) for temporary storage and transported to the laboratory within 24 hours for processing. *Cryptosporidium* spp. was detected by nested PCR of the 18S rRNA gene using primary primers F1/R1 (CCCATTTCCTTCGAAACAGGA/TTCTAGAGCTAA TACATGCG) and secondary primers F2/R2 (AAGGAGTAAGGAACAACCTCCA/GGAAGGGTTG TATTATGATAAAG). Each 25μL reaction contained 12.5μL PCR mix, 1μL DNA template, 1μL each primer, and 9.5μL water. Cycling: 95°C 5 min; 35× (95°C 15s, annealing at 55°C for primary or 58°C for secondary for 15s, 72°C 45s); 72°C 10 min. Secondary PCR used 1μL of 1:10 diluted primary product. Products were visualised on 2% agarose; positive samples showed expected bands (~830 bp primary, ~800 bp secondary) and were confirmed by Sanger sequencing. After detecting the infection of *Cryptosporidium* in fecal samples using the 18S SSU rRNA amplification and sequencing technology, the samples were divided into the *Cryptosporidium* positive group (CP, n=6) and the negative group (CO, n=6). Subsequently, fungal ITS sequence analysis was conducted on the samples of both groups separately.

Fungal ITS1 region sequencing: The internal transcribed spacer (ITS) region of fungal ribosomal DNA was selected as the target area for amplification (Sharma and Shrivastava, 2016). Fungal ITS sequencing targeted the ITS1 region using primers ITS1-F (5′-CTTGGTCATTTAGAGGAAGTAA-3′) and ITS2-R (5′-GCTGCGTTCTTCATCGATGC-3′). PCR products were purified by AMPure XP magnetic beads after verification by 2% agarose gel electrophoresis (Beckman Coulter, USA). Purified products were subjected to a second round of PCR to introduce Index sequences for constructing a sequencing library. The library was quantified using a Qubit 4.0 fluorescence quantitative instrument (Invitrogen, USA) and quality controlled using an Agilent 2100 Bioanalyzer. Then, it was sequenced on both ends on the Illumina NovaSeq PE250 platform.

Bioinformatics: The raw data after disembarking were processed using the Cutadapt software to remove the primer junction sequences, and then the double-end reads

were concatenated using the FLASH software. Quality control filtering was performed using the QIIME2 software (version 2023.2) to remove low-quality sequences (with a quality score <20, containing ambiguous bases, and having a length <200 bp). High-quality sequences were denoised, and chimeras were removed using DADA2 to generate amplicon sequence variants (ASVs). The α diversity index was calculated using QIIME2 (Usyk *et al.*, 2020), including the Chao1 index and ACE index reflecting the richness of the community, as well as the Shannon and Simpson indices reflecting the diversity of the community. In two groups, the Wilcoxon rank sum test was used to compare the differences in α diversity. The β diversity analysis was based on the Bray-Curtis distance algorithm. Through principal coordinate analysis (PCoA), differences in fungal community structure were visualized between two groups and significant variations verified using PERMANOVA permutation multivariate analysis of variance).

Differential fungus screening: The relative abundance of fungi in each sample was statistically analyzed at the phylum and genus level, and a bar chart of species composition was drawn. The LEfSe (Linear Discriminant Analysis Effect Size) method was used to screen out fungal groups that had significant differences between the two groups. All fungi with differential relative abundances were screened.

Statistical analysis: Graphpad Prism was used for all statistical analyses. Apart from the comparison of diversity, the baseline characteristics of samples in the two groups were compared using the chi-square test or Fisher's exact test, with a P<0.05 considered statistically significant.

RESULTS

Fecal fungal sequencing data: Raw image data got from fecal sequencing was converted into sequence data through base calling. The raw sequences obtained by the CP group were 72,000-136,000, and after quality control, the purified data totaled 64,000-122,000. In the CO group, a total of 74,000 - 132,000 raw sequences were discovered, and after purification, 38,000-69,000 pure sequences were obtained (Table 1). Based on the non-chimeric reads from Table 1, the total number of high-quality reads were 459,841 for the CP group and 360,148 for the CO group, with average sequencing depths of 76,640 and 60,025 reads per sample, respectively. Sequence denoising resulted in ASVs. The CP group obtained 254 ASVs (215 unique and 39 common), and the CO group obtained 351 ASVs (312 unique and 39 common) (Fig. 2A). Within the sample, the sequencing depth is sufficient to reflect all the information when the sparse curve and abundance grade curve both tend to flatten out (Fig. 1AB).

Changes in the composition of the fungal community by *Cryptosporidium* infection: The differences within the two groups were observed using alpha diversity (Chao1, ACE, Goods_coverage, Observed_species, Pielou_e, Shannon, Simpson). The significant difference between the two groups was observed in the Pieloue, Shannon, and Simpson indices (Fig. 1C). The Shannon index in the CP group has P<0.05 than in the control group (CP=2.917±0.566, CO=4.103±0.833, P=0.014). The Simpson index was also higher in the control group (CP=0.690±0.071, CO=0.867±0.098, P=0.0061). The Pielou uniformity also showed a significant decrease in the infected group (CP=0.465±0.074, CO=0.656±0.097, P=0.0039) (Table 2).

Table 1: Sequencing data analysis

SampleID	Input	Filtered	Denoised	Merged	Non-chimeric	Non-singleton
CP1	135592	130799	130647	126295	121957	121957
CP2	72930	68712	68587	67834	65093	65093
CP3	78456	73724	73584	72531	69962	69962
CP4	77010	70819	70708	69889	67565	67565
CP5	77777	67668	67550	65703	64080	64080
CP6	78397	74399	74243	73772	71184	71184
CO1	78382	72895	72721	72094	69640	69640
CO2	13182	77673	76658	72019	69345	69345
CO3	75135	40386	40242	39220	38162	38162
CO4	76392	66016	65933	64911	62318	62318
CO5	77336	68262	68019	67111	63318	63318
CO6	74797	60819	60616	59620	57365	57365

Table 2: Analysis of Alpha Diversity Indices

Sample	Chao1	ACE	Goods_coverage	Observed_species	Pielou_e	Shannon	Simpson
CP1	60	59.50893	0.9998896	58	0.3639623	2.132084	0.6335767
		9390282	64303644		76328921	8347629	84473483
CP2	77.34	77.96131	10.9999448	77	0.5655873	3.544415	00.8030064
		4754098	32151822		26129164	4297386	54311822
CP3	83	80.81585	40.9999172	80	0.5245339	3.316066	20.7274083
		5747741	48227733		96288448	0785948	37228996
CP4	74	74	1	74	0.4841788	3.006486	00.7223144
					54996396	2072374	12072899
CP5	57	57	1	57	0.4437133	2.588130	90.6331217
					1373336	5682726	20106754
CP6	83	80.99025	20.9998069	76	0.4086010	2.552910	00.6256082
		5986671	12531377		92898953	1034649	64882312
CO1	50.25	50.83924	80.9999448	50	0.6594512	3.721848	20.8748510
		6406327	32151822		92054107	5651451	09013559
CO2	62.6	64.12092	20.9999172	62	0.4768163	2.833058	30.6790351
		1400609	48227733		83537923	5159351	82676966
CO3	75	75.39064	10.9999724	75	0.7420699	4.622219	00.9403376
		9567577	16075911		36645858	9103482	75028883
CO4	84.17	84.91078	70.9999448	84	0.6572445	4.201315	90.8809200
		2431246	32151822		71817317	274546	93185409
CO5	136.2	136.7952	90.9999448	136	0.7474773	5.297717	60.9515049
		4449141	32151822		14955472	9442449	61984094
CO6	65.75	66.61819	20.9999172	65	0.6540928	3.939187	60.8754514
		627824	48227733		36439462	449055	60967934

Further analysis was conducted to examine the differences in composition between the two groups. The main fungi in both the CP and CO groups belong to Ascomycota and Basidiomycota, but the proportions of these two groups were different at the phylum level (Fig. 4CD). The Ascomycota accounted for 79.09% in the CP group and 64.82% in the CO group. The Basidiomycota accounted for 19.27% in the CP group and 15.33% in the CO group. The Neocallimastigomycota accounted for 1.58% in the CP group and 4.22% in the CO group. The proportions of Basidiomycota / Ascomycota in the two groups were basically the same, with a slight increase in the CP group. At the class level, there were some variations in proportion of fungal communities between the two groups. The Leotiomycetes content was the highest in the CP group, accounting for 61.14%, while this fungus accounted for only 7.47% in the CO group. Tremellomycetes accounted for 18.65% in the CP group and 6.36% in the CO group. Dothideomycetes accounted for 10.64% in the CP

group but was the most abundant fungus in the CO group (43.32%). Sordariomycetes accounted for 13.21% in the CO group and 4.58% in the CP group. Sordariomycetes and Ustilaginomycetes also accounted for more than 4% in the control group, but their proportions were below 1.6% in the CP group. Further analysis at the order level of fungal community changes shows that Thelebolales accounted for 61.57% in the CP group, while it only accounted for 4.75% in the CO group. The fungal genus Filobasidiales, which ranked second in the CP group (18.60%), accounted for only 5.62% in the CO group. Pleosporales accounted for 10.06% in the CP group and 39.57% in the CO group. Furthermore, in the CO group, Coniochaetales, Neocallimastigales, and Ustilaginales accounted for 6.27, 4.30, and 3.69%, respectively, but their proportions were relatively low in the CP group. At the family level, Thelebolaceae accounted for 61.8% in the CP group and 4.69% in the CO group. Filobasidiaceae was the second dominant family in the CP group, accounting for 18.66%, while it only accounted for 5.64% in the CO group. Sporormiaceae was reported as 8.75% in the CP group and 11.69% in the CO group. By analyzing the composition changes of fungal communities at the genus level, we also discovered some interesting phenomena. *Naganishia* accounted for 46.84% in the CP group, being the most abundant fungus, but only accounted for 5.91% in the CO group. The proportion of *Sporormiella* in the CP group was 10.84%, and in the CO group it was 5.46%. *Thelebolus* accounted for 9.84% in the CP group and 2.05% in the CO group. *Neoascochyta* and *Neostagonospora* were hardly detected in the CP group (0.006%, 0%), but accounted for 6.86 and 5.69% in the CO group, respectively (Fig. 2B).

The changes in the fungal community caused by *cryptosporidium* infection: β diversity can reflect the differences between sample groups. The PCoA and NMDS analyses show that the data points of the CO group and the CP group are relatively scattered, indicating a significant variation between the two groups. Based on the Jaccard distance plot (with the vertical axis representing the Beta distance), the median Beta distance of the samples between groups (Between) was 0.945, with an overall range of 0.905 to 0.960. This was significantly higher than the median of 0.845 for the samples within groups (Within) (with a range of 0.780 to 0.910), indicating that changes in microbial community structure between different groups were significantly greater than those within the overall group (Fig. 3A). The UPGMA clustering tree analysis revealed that the branch lengths between each sample in the CP group were generally short and closely clustered, indicating that the samples within the CP group had similar community structures. In the CO group, the branch lengths between some samples were relatively longer, and the branch structure was more dispersed, suggesting that there were certain differences among the samples in the CO group. Overall, the UPGMA clustering results showed that samples in the CP and CO groups could be clearly separated (Fig. 3B). The cladogram analysis reflects the relative abundance. The characteristic microorganisms at the class level related to the CO group mainly include Dothideomycetes, Pleosporales at the order level, Didymellaceae at the family level, etc. While Leotiomycetes at the class level and Thelebolales at the family level are characteristic microorganisms of the CP group (Fig. 4A).

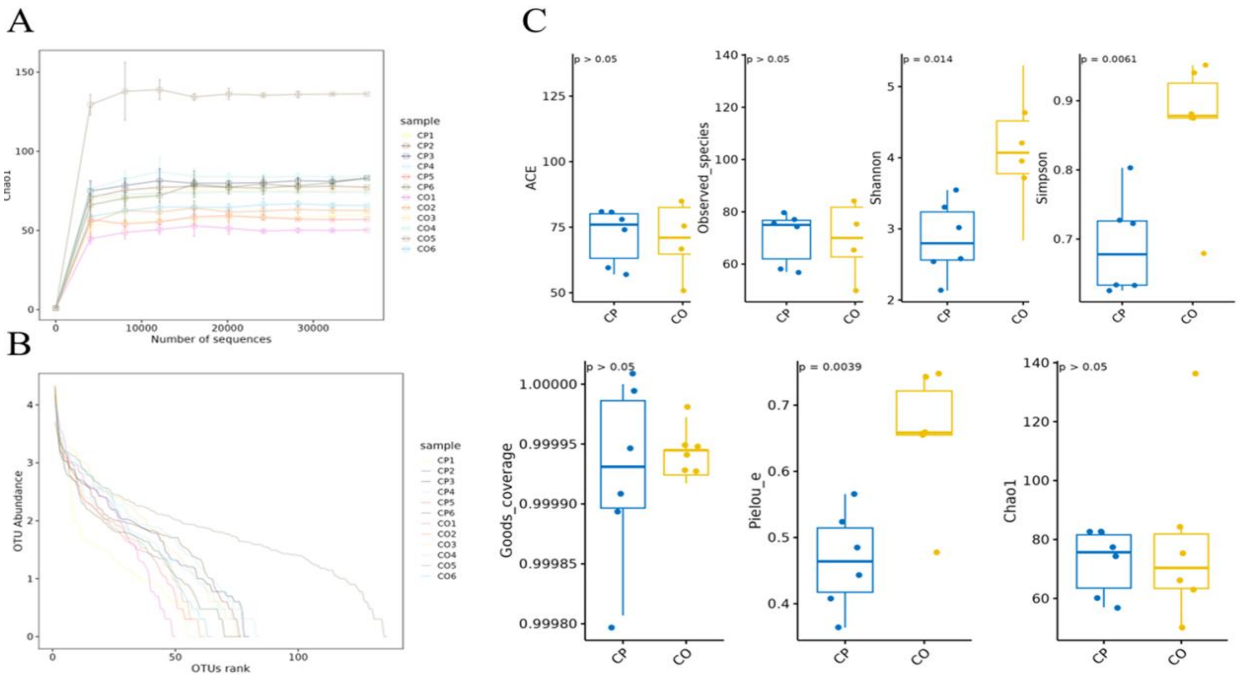

Fig. 1: The impact of *Cryptosporidium* infection on the alpha diversity of intestinal fungi. A: Sparse curve (The gentler the curve, the more it indicates that the sequencing results have adequately reflected the diversity contained in the current sample). B: Abundance grade curve (the smoothness of the line reflects the evenness of the community composition). C: Alpha diversity analysis (Chao1, ACE and Observed species indices represent richness, Shannon and Simpson indices represent diversity, Faith's PD index represents evolutionary-based diversity, Pielou's evenness index represents evenness, and Good's coverage index represents coverage). Data are presented as mean ± SEM.

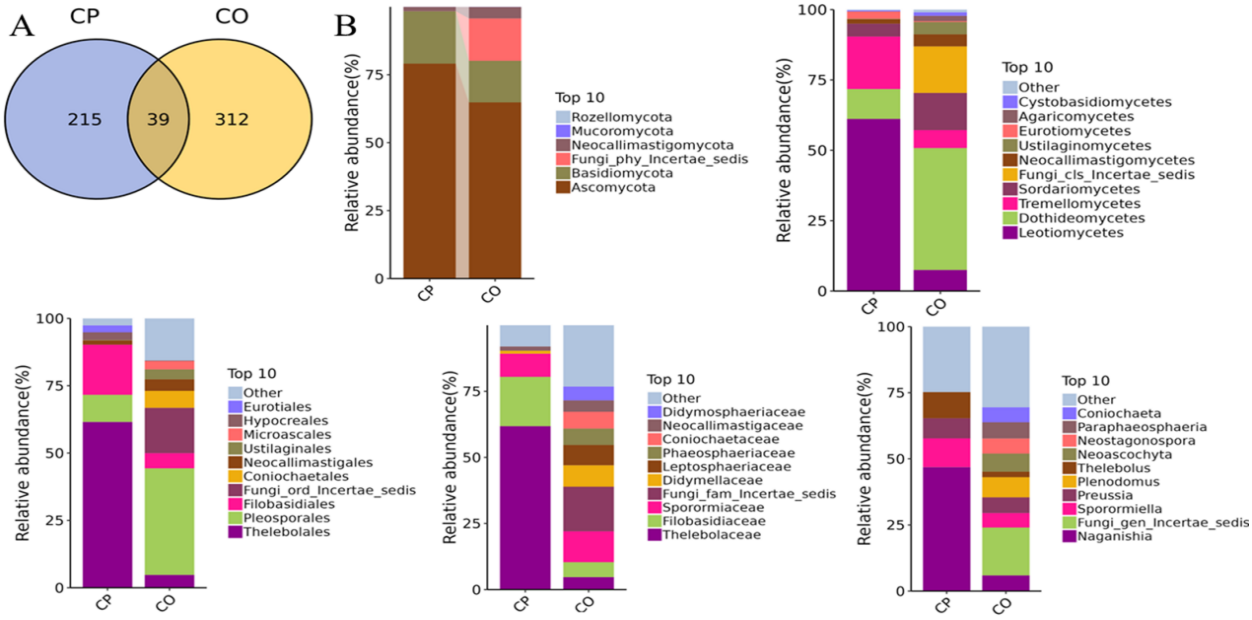

Fig. 2: The impact of *Cryptosporidium* infection on the composition of the intestinal fungal community. A: Venn diagram of ASVs. B: Composition of intestinal fungal communities at different classification levels (Phylum, Class, Order, Family, Genus).

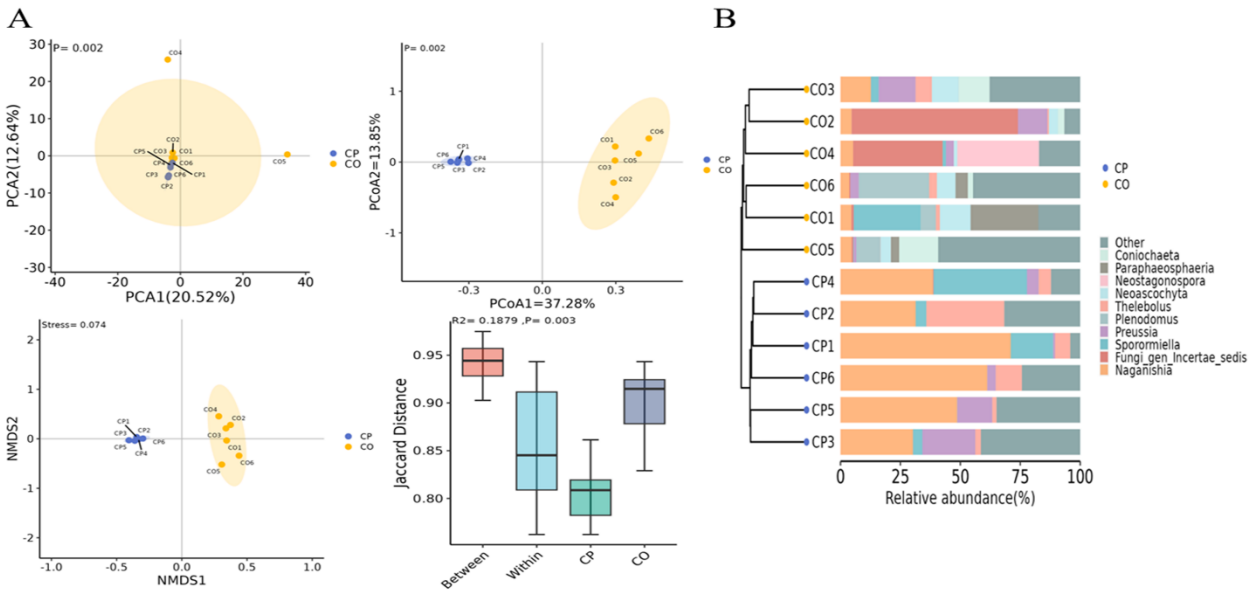

Fig. 3: The impact of *Cryptosporidium* infection on the composition of intestinal fungi. A: Beta diversity analysis, including Principal Component Analysis (PCA), Principal Coordinate Analysis (PCoA), and Nonmetric Multidimensional Scaling (NMDS). B: UPGMA clustering analysis.

The Wilcox test was used to further analyze the variations in fungi between the two groups. At the class level, the relative abundances of Dothideomycetes, Ustilaginomycetes and Walleronycetes in CO group were significantly higher than CP group, while Leotiomycetes and Tremellomycetes were enriched in CP group significantly and their relative abundances also significantly higher than in group CO (Fig. 5A). At order level, the relative incidence of Coniochaetales and Pleosporales in CO group was significantly higher than those in CP group; while Eurotiales, Filobasidiales, Thelebolales, and Wallemiales were significantly enriched in the CP group and their relative abundances were significantly higher than those in the CO group (Fig. 5B). In genus level analysis of the differences, relative abundances of *Neoascochyta*, *Coniochaeta*, and unnamed genus Fungi-genincerta-seeds in CO group showed significant difference than in CP group, while *Naganisha*, *Aspergillus*, *Cyllamyces*, and *Neocallimastixt* were significantly higher in CP group and their relative abundances were significantly higher than those in the CO group (Fig. 5C). According to the volcano plot results of ZicoSeq differential analysis, the significantly different ASVs/OTUs include ASV_268 (Neoascochyta), ASV_255 (Thelebolaceae), ASV_437 (Thelebolaceae), ASV_388 (Naganishia albida), ASV_63 (Neocallimastigaceae), ASV_251 (Cleistothelebolus nipigonensis), ASV_477 (Neocallimastigaceae), ASV_486 (Piromyces_sp), ASV_507 (Neocallimastigaceae) and ASV_156 (Aspergillus ruber). The results of the volcano plot analysis were basically consistent with those of the difference comparison (Table 3, Fig. 5D).

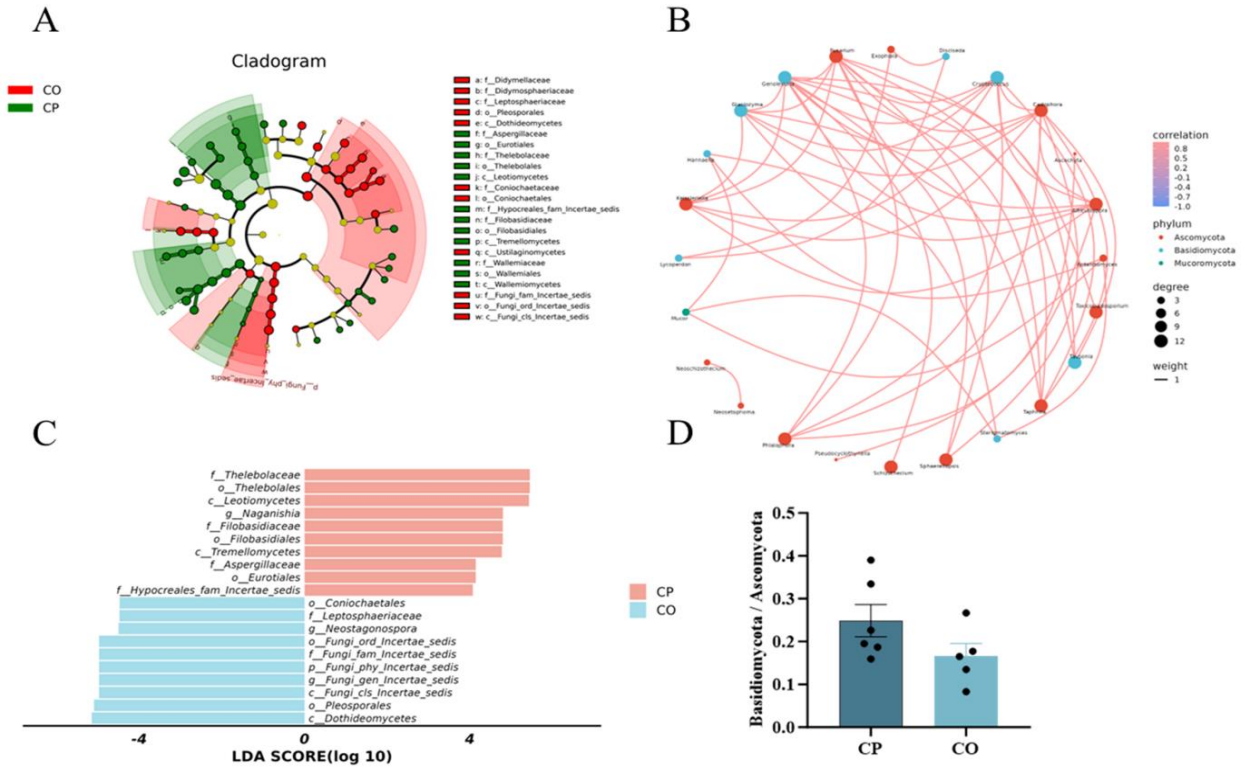

Fig. 4: Analysis of differences in intestinal fungal species caused by *Cryptosporidium* infection. A: Evolutionary Branch Diagram. B: Graph of genus-level association network. C: Bar chart of LDA effect values for indicator species (genus). D: Proportions of Basidiomycota / Ascomycota.

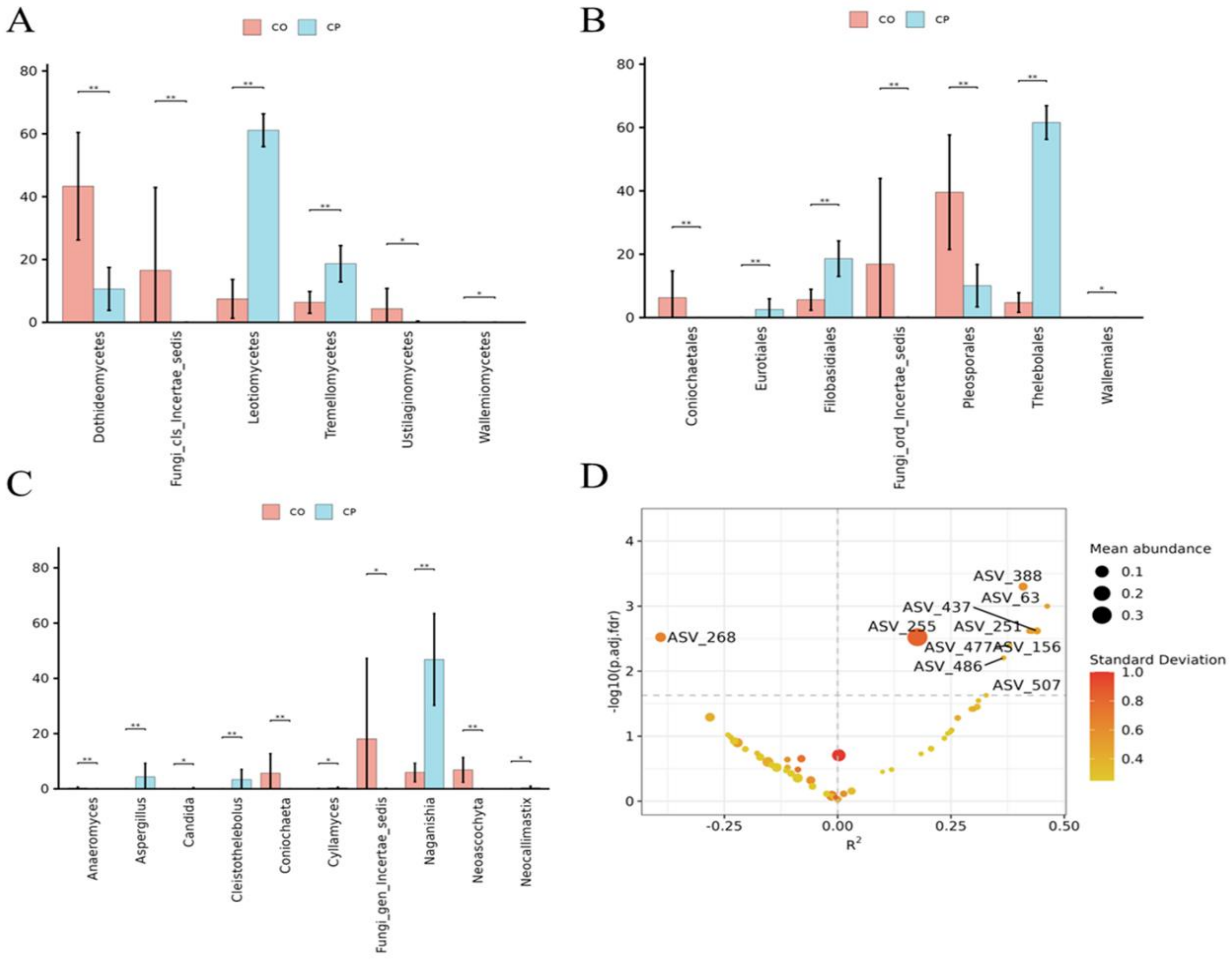

Fig. 5: Analysis of intestinal fungal marker species caused by *Cryptosporidium* infection. A: Class-level Kruskal-Wallis rank sum test. B: Order-level Kruskal-Wallis rank sum test. C: Kruskal-Wallis rank sum test at the genus level. D: Volcano plot based on ZicoSeq differential ASV/OUT. Statistical significance is indicated as *P<0.05, **P<0.01. Data are presented as mean ± SEM.

Table 3: Difference volcano plot data

ASV_ID	Mean	R2	p.value	p.adj.fdr	p.adj.fwer	taxonomy
ASV_388769.916666666667	0.409211976270136	0.001	0.0005005005005005	0.001	d__Fungi; p__Basidiomycota; c__Tremellomycetes; o__Filobasidiales; f__Filobasidiaceae; g__Naganishia; s__Naganishia_albida
ASV_63	42.91666666666670.462383452920619	0.002	0.001001001001001	0.002	d__Fungi; p__Neocallimastigomycota; c__Neocallimastigomycetes; o__Neocallimastigales; f__Neocallimastigaceae
ASV_437381.583333333333	0.439692175215196	0.001	0.0024024024024024	0.008	d__Fungi; p__Ascomycota; c__Leotiomycetes; o__Thelebolales; f__Thelebolaceae
ASV_2559876.166666666667	0.175960063235742	0.004	0.003003003003003	0.012	d__Fungi; p__Ascomycota; c__Leotiomycetes; o__Thelebolales; f__Thelebolaceae
ASV_268818.166666666667	0.390647670135774	0.001	0.003003003003003	0.012	d__Fungi; p__Ascomycota; c__Dothideomycetes; o__Pleosporales; f__Didymellaceae; g__Neoascochyta
ASV_437381.583333333333	0.439692175215196	0.001	0.0024024024024024	0.008	d__Fungi; p__Ascomycota; c__Leotiomycetes; o__Thelebolales; f__Thelebolaceae
ASV_251203.75	0.428077296137067	0.002	0.0024024024024024	0.009	d__Fungi; p__Ascomycota; c__Leotiomycetes; o__Thelebolales; f__Thelebolaceae; g__Cleistothelebolus; s__Cleistothelebolus_nipigonensis
ASV_47722.833333333333	0.37950278659848	0.01	0.004004004004004	0.022	d__Fungi; p__Neocallimastigomycota; c__Neocallimastigomycetes; o__Neocallimastigales; f__Neocallimastigaceae
ASV_156133.5	0.423092996801438	0.002	0.0024024024024024	0.009	d__Fungi; p__Ascomycota; c__Eurotiomycetes; o__Eurotiales; f__Aspergillaceae; g__Aspergillus; s__Aspergillus_ruber
ASV_48629	0.366052193826287	0.004	0.006228450672895	120.025	d__Fungi; p__Neocallimastigomycota; c__Neocallimastigomycetes; o__Neocallimastigales; f__Neocallimastigaceae; g__Piromyces; s__Piromyces_sp
ASV_50718.333333333333	0.327557165579866	0.047	0.0235235235235235	0.1	d__Fungi; p__Neocallimastigomycota; c__Neocallimastigomycetes; o__Neocallimastigales; f__Neocallimastigaceae

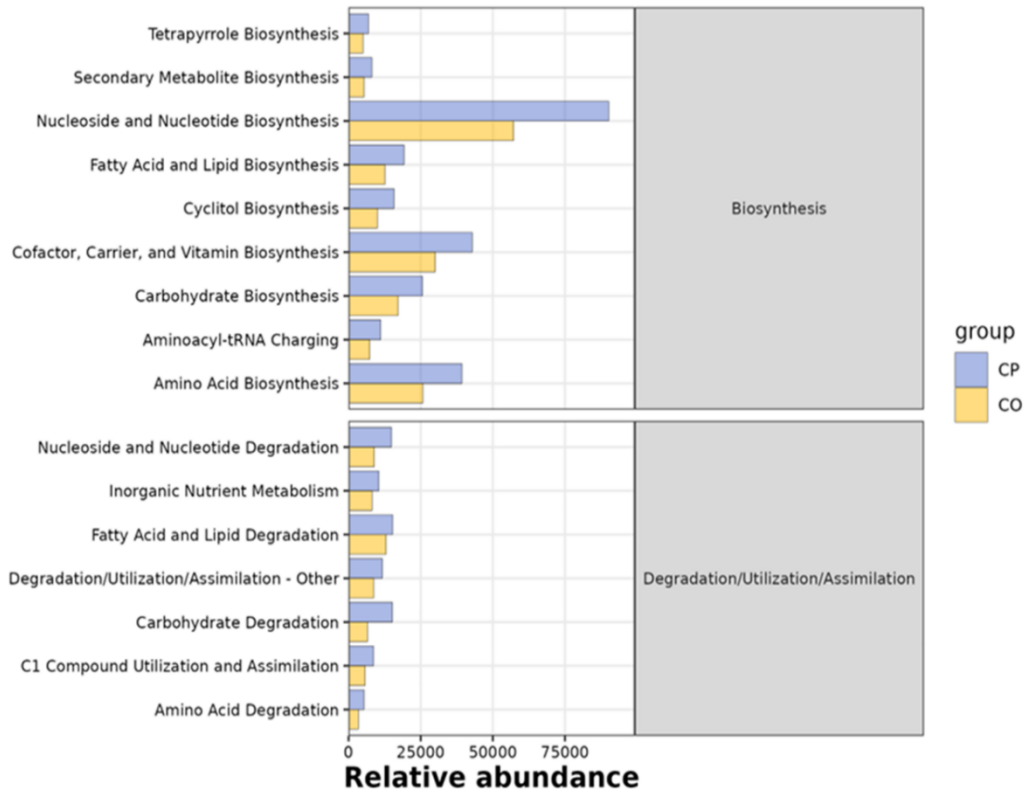

Fig. 6: The abundance graph of the MetaCyc secondary functional pathways of the changed intestinal fungi.

The horizontal correlation network diagram shows the correlations among the fungi. The abundances of Mucor, Cryptococcus, Cadophora, etc., are relatively high, and these fungi have strong correlations with many other genera in the network (Fig. 4B).

Statistics of fungal metabolic pathways: Among the predicted functions of the microbial community, all the listed MetaCyc secondary functional pathways (including tetra-pyrrole biosynthesis, secondary metabolite biosynthesis, nucleotide and nucleoside biosynthesis, fatty acid and lipid biosynthesis, cyclic alcohol biosynthesis, cofactor/transporter/vitamin biosynthesis, carbohydrate biosynthesis, aminoacyl-tRNA connection, amino acid biosynthesis, as well as various degradation and utilization pathways) had higher abundances in the CP group (Fig. 6).

DISCUSSION

Cryptosporidium is one of the major pathogens causing diarrhea worldwide (Wojcik *et al.*, 2020; Bergholm *et al.*, 2024), mainly infecting the epithelial cells of the gastrointestinal tract and disrupting the host's intestinal microecology. Studies have shown that the intestinal fungal communities play a significant role in the host's intestinal homeostasis and disease progression (Leonardi *et al.*, 2022; Zhang *et al.*, 2022), the impact of *Cryptosporidium* infection on the intestinal fungal communities has not been fully understood.

The results of the alpha diversity analysis indicate that the Shannon and Simpson indices of the infection group (CP group) were significantly lower than those of the control group (CO group), and the Pielou evenness also showed the same trend. The Shannon and Simpson indices comprehensively reflect species richness and evenness (Su *et al.*, 2024), and their significant decrease suggests that *Cryptosporidium* infection leads to a decrease in the diversity and evenness of the intestinal fungal communities, with some dominant groups proliferating excessively and the community balance being disrupted (Sadia *et al.*, 2024). Previous studies have also observed that the composition and proportion of the intestinal fungal communities change significantly after *Cryptosporidium* infection, and the abundance of beneficial fungi decreases. Notably, both the sparse curve and the abundance grade curve tend to be flat, indicating that sequence depth is enough to reflect the overall microorganisms within the sample, and the sequencing data is reliable. Beta diversity analysis shows that the median Jaccard distance between groups is significantly higher than that within groups, and the UPGMA clustering tree diagram clearly separates the samples of the CP group and the CO group, indicating that *Cryptosporidium* infection has a significant impact on the overall structure of the intestinal fungal communities (Segura-Alabart *et al.*, 2022), and the two groups have already shown significant differences in community composition.

At the phylum level, both the CP group and the CO group were dominated by the Ascomycota and Basidiomycota phyla, which are in line with the basic characteristics of the fungal communities in animal intestines. However, there were significant differences in the proportions between the two groups. The relative abundance of the Ascomycota phylum in the CP group (79.09%) was greater than that in the CO group (64.82%), while the incidence of the Basidiomycota phylum in the CO group was relatively lower. Studies have shown that changes in the ratio of the Ascomycota phylum to the Basidiomycota phylum in the intestinal tract may be related to the intestinal inflammatory state (Sokol *et al.*, 2017; Li *et al.*, 2018). In patients with intestinal diseases, an increase in the ratio of the Basidiomycota phylum to the Ascomycota phylum is often observed (Yadav *et al.*, 2022). Previously, in the intestines of patients with ankylosing spondylitis (a disease accompanied by subclinical intestinal inflammation), an increase in the level of the Ascomycota phylum, especially the Dothideomycetes, and a decrease in the Basidiomycota phylum were also found (Li *et al.*, 2019). The increased relative abundance of Ascomycota in the CP group could reflect intestinal inflammatory changes, as similar shifts have been observed in other inflammatory conditions; however, direct causal evidence in our model is lacking and requires further investigation.

A further analysis of the changes at the lower classification levels revealed that the negative effects caused by infection were more evident. In the CP group, the abundances of *Neoascochyta* and *Neostagonospora* were very low (with relative abundances of only 0.006% and 0%, respectively), while these two genera accounted for 6.86 and 5.69%, respectively, in the CO group. Both *Neoascochyta* and *Neostagonospora* are common plant pathogenic fungi (Marin-Felix *et al.*, 2019; Kinnunen-Grubb *et al.*, 2020), and they may enter the intestinal tract along with the feed. The sharp decrease in the abundance of these exogenous fungi in the CP group is likely due to the reduced appetite and decreased feed intake of the infected animals. *Thelebolaceae* had a relative abundance of 61.8% in the CP group, which was much higher than 4.69% in the CO group. In the study on the fungal diversity of wild bison intestines, *Thelebolus* was one of the dominant genera (accounting for 30.93% of the total abundance), and some strains of this genus were confirmed to have pathogenic properties. Ma *et al*. (2024) further pointed out that certain strains of *Thelebolus*, *Cryptococcus*, *Trichosporon*, and *Candida* among the genera identified in the feces of wild bison all had pathogenic potential. In the CP group at the genus level, the relative abundance of Naganishia was as high as 46.84%, while it was only 5.91% in the CO group. Although *Naganishia* is common in the intestines of healthy animals, it is also an important opportunistic pathogenic fungus that can cause fatal fungal sepsis and central nervous system infections in immunosuppressed hosts (Choe *et al.*, 2020). *Naganishia albida* (also known as *Cryptococcus albidus*) is an opportunistic yeast that can cause life-threatening fungal sepsis and central nervous system infections in individuals with compromised immune function. Studies have clearly demonstrated that *C. albidus* is an opportunistic fungus that can cause life-threatening infections in individuals of any age, especially in those with compromised immune function (Thomson *et al.*, 2017; Brito *et al.*, 2019). The functional prediction analysis revealed that the average abundance of all the listed MetaCyc secondary functional pathways in the CP group was slightly higher than that in the CO group. Since the functional potential prediction analysis is based on species composition data for calculation, the high enrichment of a few groups, such as *Naganishia* in the CP group, may have had a significant impact on the overall functional estimation value. This does not necessarily mean that the metabolic contribution of the microbial community to the host has been enhanced. These changes in fungal abundance suggest that the changes in the intestinal microenvironment after *Cryptosporidium* infection may provide conditions for the proliferation of these fungi with potential pathogenicity. This study shows that the alpha diversity of the intestinal fungal community significantly decreased after *cryptosporidium* infection, and the composition of the community changed significantly. There were also significant differences between the CP group and the CO group at multiple taxonomic levels, including phylum, class, order, and genus.

Conclusions: Based on the above results, the intestinal fungi changed at multiple taxonomic levels after *Cryptosporidium* infection. The diversity and evenness of fungi in the infected group significantly decreased. In terms of specific fungal composition, the infected group was characterized by the enrichment of fungi such as Leotiomycetes, Thelebolales, *Thelebolaceae*, and *Naganishia*, while the control group was enriched Dothideomycetes, Pleosporales, *Coniochaetales*, and *Neoascochyta*. The Wilcox test further confirmed the statistical significance of these differences at the phylum, class, and genus levels. A significant increase in opportunistic fungi *Naganishia* and *Thelebolaceae,* in the infected group suggested that *Cryptosporidium* infection might simultaneously affect the host's immunity and the digestive and metabolic functions of the intestine. These changes in fungal communities provide a new perspective for understanding the related intestinal microecological changes during *Cryptosporidium* infection.

Data Availability: All the raw data sequences from animals were deposited in the NCBI Sequence Read Archive database under the accession number: PRJNA1473677.

Ethics statement: Laboratory Animals Research Centre of Jiangsu, China, and the ethics committee of Nanjing Agricultural University gave ethical approval, and all experimental operations were performed under the instructions (NJAU.No20240910164).

Author contributions: BS: research idea and methodology; BS, CX, CZ: reagents, materials, and analysis tools; BS, MHA: writing – original draft and preparation, writing – review and editing; BS: visualization and supervision; All authors approved the final manuscript for publication.

Funding: This study was supported by the Project of the Science and Technology Program of Xizang, China (XZ202601ZY0136-3), and Base and Talent Project of the Science and Technology Program of Xizang, China (XZ202401JD0012).

Acknowledgement: The authors extend their appreciations to the Ongoing Research Funding Program (ORF-2026-191), King Saud University, Riyadh, Saudi Arabia.

REFERENCES

Adkins PRF, 2022. Cryptosporidiosis. Veterinary Clinics of North America in Food Animal Practice 38:121-131.

Alberfkani MI, Swar SO, Almutairi LA, *et al.,* 2024. Molecular characterization and phylogenetic analysis of 18s rRNA, gp60 and HSP70 genes of Cryptosporidium parvum isolate d from cattle owners and cattle using nested PCR. Pakistan Veterinary Journal 44(4):1237-1242.

Bergholm J, Tessema TS, Blomström AL, *et al.*, 2024. Detection and molecular characterization of major enteric pathogens in calves in central Ethiopia. BMC Veterinary Research 20:389.

Bouzid M, Hunter PR, Chalmers RM, *et al.*, 2013. *Cryptosporidium* pathogenicity and virulence. Clinical Microbiology Reviews 26:115-134.

Brito M de O, Bessa MA de S, Menezes R de P, *et al.*, 2019. Isolation of Cryptococcus species from the external environments of hospital and academic areas. The Journal of Infection in Developing Counttries 13:545-553.

Budu-Amoako E, Greenwood SJ, Dixon BR, *et al.*, 2011. Foodborne illness associated with *Cryptosporidium* and *Giardia* from livestock. Journal of Food Protection 74:1944-1955.

Chen Y, Han B, Guan X, *et al.*, 2024. Enteric fungi protect against intestinal ischemia-reperfusion injury via inhibiting the SAA1-GSDMD pathway. Journal of Advanced Research 61:223-237.

Choe YJ, Blatt DB, Yalcindag A, *et al.*, 2020. *Cryptococcus albidus* Fungemia in an Immunosuppressed Child: Case Report and Systematic Literature Review. Journal of Pediatric Infectious Disease Society 9:100-105.

Dong H, Chen X, Zhao X, *et al.*, 2023. Intestine microbiota and SCFAs response in naturally *Cryptosporidium*-infected plateau yaks. Frontiers in Cellular and Infection Microbiology 13:1105126.

Geng HL, Ni HB, Li JH, *et al.*, 2021. Prevalence of *Cryptosporidium* spp. in Yaks (Bos grunniens) in China: A Systematic Review and Meta-Analysis. Frontiers in Cellular and Infection Microbiology 11:770612.

Guo Y, Ryan U, Feng Y, *et al.*, 2022. Emergence of zoonotic *Cryptosporidium parvum* in China. Trends in Parasitology 38:335-343.

Harp JA, 2003. *Cryptosporidium* and host resistance: historical perspective and some novel approaches. Animal Health Research Reviews 4:53-62.

Hatter JA, Kouche YM, Melchor SJ, *et al.*, 2018. *Toxoplasma gondii* infection triggers chronic cachexia and sustained commensal dysbiosis in mice. PLoS One 13:e0204895.

Hertli S and Zimmermann P, 2022. Molecular interactions between the intestinal microbiota and the host. Molecular Microbiology 117:1297-1307.

Ichikawa-Seki M, Motooka D, Kinami A, *et al.*, 2019. Specific increase of Fusobacterium in the faecal microbiota of neonatal calves infected with *Cryptosporidium parvum*. Scientific Reports 9:12517.

Ignatiou A and Pitsouli C, 2024. Host-diet-microbiota interplay in intestinal nutrition and health. FEBS Letters 598:2482-2517.

Ji Y, Ali M, Xu C, *et al.*, 2025. Epidemiological Exploration of *Cryptosporidium* spp., *Giardia intestinalis*, Enterocytozoon bieneusi, and Blastocystis spp. in Yaks: Investigating Ecological and Zoonotic Dynamics in Lhasa, Xizang. Veterinary Science 12(5):504.

Kinnunen-Grubb M, Sapkota R, Vignola M, *et al.*, 2020. Breeding selection imposed a differential selective pressure on the wheat root-associated microbiome. FEMS Microbiology and Ecology 96:fiaa196.

Leonardi I, Gao IH, Lin W-Y, *et al.*, 2022. Mucosal fungi promote gut barrier function and social behavior via Type 17 immunity. Cell 185:831-846.e14.

Li J, Chen D, Yu B, *et al.*, 2018. Fungi in gastrointestinal tracts of human and mice: from Community to Functions. Microbiology and Ecology 75:821-829.

Li M, Dai B, Tang Y, *et al.*, 2019. Altered bacterial-fungal interkingdom networks in the guts of ankylosing spondylitis patients. mSystems 4(2):e00176-18.

Lin G, Ou W, Yang J, *et al.*, 2025. Correlation of intestinal bacteria, fungi and dietary nutrient intake in NAFLD patients with spleen deficiency syndrome. Frontiers in Cellular and Infection Microbiology 15:1586212.

Lu S, Zou W, Chen X, *et al.*, 2023. Effects of *Cryptosporidium parvum* infection on intestinal fungal microbiota in yaks (*Bos grunniens*). Microbial Pathogenesis 183:106322.

Ma X, Li Z, Cai L, *et al.*, 2024. Analysis of fungal diversity in the gut feces of wild takin (*Budorcas taxicolor*). Frontiers in Microbiology 15:1364486.

Marin-Felix Y, Hernández-Restrepo M, Iturrieta-González I, *et al.*, 2019. Genera of phytopathogenic fungi: GOPHY 3. Students Mycology 94:1-124.

Peng S, Xu C, Saleem MU, *et al.,* 2024. Epidemiological investigation of Cryptosporidium infection in yaks in chamdo, China. Pakistan Veterinary Journal 44(2):535-538.

Sadia S, Waheed M, Firdous S, *et al.*, 2024. Ecological analysis of plant community structure and soil effects in subtropical forest ecosystem. BMC Plant Biology 24:1275.

Segura-Alabart N, Serratosa F, Gómez S, *et al.*, 2022. Nonunique UPGMA clusterings of microsatellite markers. Brief Bioinformatics 23(5):bbac312.

Shah AM, Bano I, Qazi IH, *et al.*, 2023. "The Yak"-A remarkable animal living in a harsh environment: An overview of its feeding, growth, production performance and contribution to food security. Frontiers in Veternary Science 10:1086985.

Sharma S and Shrivastava N, 2016. Internal transcribed spacer guided multiplex PCR for species identification of *Convolvulus prostratus* and

Evolvulus alsinoides. Acta Pharmaceutica Sinica B 6:253-258.

Shehata AA, El-Emam MMA, Gouda H, *et al.,* 2024. Molecular characterization of Cryptosporidium parvum infections and analysis of hemological and biochemical changes in diarrheic pre-weaned calves in Egypt. Pakistan Veterinary Journal 44(1):135-140.

Sokol H, Leducq V, Aschard H, *et al.*, 2017. Fungal microbiota dysbiosis in IBD. Gut 66:1039-1048.

Soliman N, Kruithoff C, San Valentin EM, *et al.*, 2025. Small intestinal bacterial and fungal overgrowth: Health implications and management perspectives. Nutrients 17(8):1365.

Su QY, Zhang Y, Qiao D, *et al.*, 2024. Gut microbiota dysbiosis in ankylosing spondylitis: a systematic review and meta-analysis. Frontiers in Cellular and Infection Microbiology 14:1376525.

Thomson P, Mayayo E, López-Fernández L, *et al.*, 2017. Combined antifungal therapy against systemic murine infections by rare Cryptococcus species. Mycoses 60:112-117.

Usyk M, Zolnik CP, Castle PE, *et al.*, 2020. Cervicovaginal microbiome and natural history of HPV in a longitudinal study. PLoS Pathogens 16:e1008376.

Wang D and Zeng J, 2026. Microbiome analysis reveals the adverse effects of diarrhea on the gut microbiota of yaks. Microbial Pathogenesis 211:108218.

Wojcik GL, Korpe P, Marie C, *et al.*, 2020. Genome-wide association study of Cryptosporidiosis in infants implicates PRKCA. mBio 11(1):e03343-19.

Xu C, He Q, Zhu Z, *et al.*, 2025. Propolis improves intestinal barrier function against *Cryptosporidium parvum* via NLRP6 inflammasome. mBio 16:e0231725.

Yadav M, Ali S, Shrode RL, *et al.*, 2022. Multiple sclerosis patients have an altered gut mycobiome and increased fungal to bacterial richness. PLoS One 17:e0264556.

Zhang F, Aschenbrenner D, Yoo JY, *et al.*, 2022. The gut mycobiome in health, disease, and clinical applications in association with the gut bacterial microbiome assembly. Lancet Microbe 3:e969-e983.